Research Article

Journal of Physical Organic Chemistry

Received: 28 May 2008, Revised: 18 August 2008, Accepted: 11 October 2008, Published online in Wiley InterScience: 8 December 2008

(www.interscience.wiley.com) DOI 10.1002/poc.1475

A metal free blue emission by the protonated 2,2′:6′,2″-terpyridine hexafluorophosphate

Naokazu Yoshikawa[a]*, Shinichi Yamabe[b], Nobuko Kanehisa[c], Hiroshi Takashima[a] and Keiichi Tsukahara[a]

Mono-protonated 2,2′:6′,2″-terpyridine (terpy) compound, 2,2′:6′,2″-terpyridinium hexafluorophosphate {[terpyH]PF_6}, was prepared and characterized by electrospray ionization mass spectrometry, UV–Vis and emission spectroscopies, cyclic voltammogram (CV), and X-ray crystallography. The proton is located at the central pyridine nitrogen atom of terpy and was found in electron density difference map, which is completely different from the previously reported mono-protonated species, such as [terpyH]ReO_4 and [terpyH]CF_3SO_3. The H^+ in the latter species is located at the terminal pyridine nitrogen. A small difference of proton positions was found to give a drastic difference of crystal patterns. For [terpyH]PF_6 in CH_3CN, a new π–π^* band in the UV region and a blue emission ($\Phi = 0.052$ at room temperature) appeared whose maxima were red-shifted relative to those of the corresponding neutral terpy ligand. CV for the proton adduct showed the first reduction wave at around −0.6 V, being more positive than that of the neutral species. Finally, the density-functional theory (DFT) approach was used to investigate isomerization processes of the protonated terpy. Copyright © 2008 John Wiley & Sons, Ltd.

Keywords: terpyridine; emission; aggregation pattern; DFT calculation

INTRODUCTION

The chemistry of 2,2′:6′,2″-terpyridine (terpy) complexes has significantly expanded in recent years, and particular attention has been focused on ruthenium(II) complexes because of their attractive photochemical and electrochemical properties. The luminescence lifetime at room temperature is 36 ns and luminescence quantum yield is 4×10^{-4} for [Ru(terpy-SO_2Me)(terpy)]$^{2+}$ {terpy-SO_2Me = 4′-(methylsulfonyl)-2,2′:6′,2″-terpyridine}.[1] Although terpyridine-Ru^{II} complexes tend both to have a relatively short-lived excited triplet state of the metal-to-ligand charge transfer (^{3}MLCT) and to be weak emitters, rational strategies can be devised to increase the excited-state lifetime of the terpyridine-Ru^{II} complexes.[2–5]

The free terpy ligand has a nonplanar geometry. Upon protonation of the pyridine-N atom of terpy, the extension of the π delocalization in terpy can be expected. It was reported that the doubly protonated terpyridinium and tetra-2-pyridyl-pyrazinium (peripheral pyridine-N atoms, N1 and N3) cations could be easily prepared so far and theoretical and experimental studies of these structures have also been carried out.[6–8] However, 2,2′:6′,2″-terpyridinium compounds formed by protonation at the central pyridine nitrogen atom of terpy are generally difficult to prepare. Therefore, we tried to synthesize and evaluate the emission property of this type of compound. In this work, we obtained the crystal structure of [terpyH]PF_6, of which the terpyH moiety has a planar geometry (Scheme 1) and shows an intense blue emission without a central metal ion, such as ruthenium(II). The effect of protonation on its photophysical and electrochemical properties and the crystal pattern was investigated.

EXPERIMENTAL

Reagents

Terpy, potassium hexafluorophosphate (KPF_6), ruthenium(III) trichloride monohydrate ($RuCl_3 \cdot H_2O$), and tetrabutylammonium perchlorate (TBAP) were purchased from Aldrich and used without further purification. Acetonitrile (CH_3CN) used in the spectroscopic and electrochemical measurements was of spectroscopic grade from Dojindo Laboratory. [terpyH]PF_6 was synthesized for the first time by modification of our previous procedure.[9]

Synthesis of the mono-protonated compound [terpyH]PF_6

[terpyH]PF_6 was obtained during the following synthesis for the Ru^{II}-terpy complex. Terpy (0.117 g, 0.500 mmol) and $RuCl_3 \cdot H_2O$

* *Correspondence to: N. Yoshikawa, Department of Chemistry, Faculty of Science, Nara Women's University, Nara 630-8506, Japan.*
E-mail: naokazuu@dream.com

a *N. Yoshikawa, H. Takashima, K. Tsukahara*
Department of Chemistry, Faculty of Science, Nara Women's University, Nara 630-8506, Japan

b *S. Yamabe*
Department of Chemistry, Nara University of Education, Nara 630-8528, Japan

c *N. Kanehisa*
Department of Applied Chemistry, Graduate School of Engineering, Osaka University, Osaka 565-0871, Japan

Journal of Physical Organic Chemistry

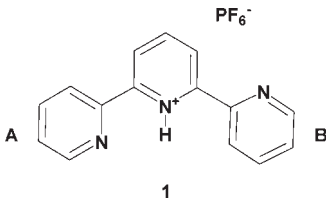

1

Scheme 1. Structural formulae of the protonated terpy and hexafluorophosphate anion. Two pyridine rings are called here A and B for explanations

(0.113 g, 0.500 mmol) were mixed in ethylene glycol (15 ml) and the suspended mixture was refluxed for 5 min in a microwave oven (Mitsubishi; RR-12AF; 500 W, 2450 MHz).[10,11] After the reaction mixture was cooled to room temperature, the saturated aqueous solution of KPF_6 (20 ml) was added. A slightly yellow crystal was obtained as terpyridinium hexafluorophosphate (yield: 10%).

[terpyH]PF_6 found: C, 46.70; H, 3.12; N, 11.10%. Calcd for $C_{15}H_{12}N_3PF_6{\cdot}0.5H_2O$: C, 46.37; H, 3.09; N, 10.82%. ^{1}H NMR (CD_3CN): δ/ppm = 7.90 (dd, 2H, J = 6.4 Hz), 8.42 (dd, 1H, J = 8.0 Hz), 8.46 (dd, 2H, J = 8.0 Hz), 8.65 (d, 2H, J = 8.0 Hz), 8.81 (d, 2H, J = 8.0 Hz), 8.92 (d, 2H, J = 4.8 Hz). ESI-MS ([terpyH]PF_6 in CH_3CN, positive): m/z = 234.14 ([terpyH]$^+$ requires 234.27).

Measurements

Electronic absorption spectra of neutral and protonated compounds were recorded at room temperature in CH_3CN solution with a Shimadzu UV-2550 spectrophotometer. ESI-Mass spectra were obtained by a JEOL JMS-T100LC AccuTOF spectrometer. NMR spectra were recorded on a JEOL JNM-AL400 FT-NMR. ^{1}H NMR chemical shift values are reported in ppm as reference to the internal standard TMS in CD_3CN solution. Cyclic voltammogram (CV) was measured on an ALS-610B electrochemical analyzer fitted with a three-electrode system consisting of a glassy carbon working electrode, a platinum auxiliary electrode, and a Ag/AgCl reference electrode (+0.21 V *vs*. NHE at 3.5 M KCl). CV experiments were performed for CH_3CN solution of the compound (5.0×10^{-4} M) and 0.050 M TBAP under nitrogen atmosphere with a scan rate of 0.1 V s^{-1}. The emission spectrum and lifetimes were measured in nitrogen-equilibrated CH_3CN solutions using a Shimadzu RF5300 fluorimeter and a Horiba single-photon counting system (NAES-500). The emission quantum yield for the protonated terpy were determined in CH_3CN at room temperature relative to those of a solution containing $[Ru(bpy)_3]^{2+}$ and having the same absorbance.

Crystallographic data collection and structure determination

The X-ray measurement was made on a Rigaku R-Axis-Rapid Imaging Plate diffractometer with graphite monochromated MoKα radiation.[11] Indexing was performed from three oscillations. The camera radius was 127.40 mm. Readout was performed in the 0.100 mm pixel mode. The structure was solved by direct methods and refined on F^2 by full-matrix least-squares methods, using SHELXL-97.[12] The non-hydrogen atoms were refined anisotropically by the full-matrix least-squares method. All hydrogen atoms were isotropically refined. We attempted to improve R value. However, we could not obtain smaller one.

Computational methods

The density-functional theory (DFT) calculations of free terpy and its protonated compound (except PF_6^-) were performed using the Gaussian98 program package.[13] The Becke three parameters hybrid exchange[14] and the Lee–Yang–Parr correlation functionals (B3LYP)[15] were used. Geometry optimizations and subsequent vibrational analyses were performed by B3LYP/6-31G*. Subsequent single-point energy calculations were made by B3LYP/6-311+G(3df, 2p) and relative energies of the protonated terpy were obtained by the B3LYP/6-31G* zero-point vibrational energies and B3LYP/6-31+G(3df, 2p) electronic energies. The B3LYP/6-311+G(3df, 2p)//B3LYP/6-31G* is known to give reliable energies.[16] ^{1}H NMR chemical shifts were evaluated by RHF/6-311+G(2d, p) GIAO calculations[17] with the solvent effect, SCRF = PCM.[18]

RESULTS AND DISCUSSION

Crystal structure

[terpyH]PF_6 was obtained from the reaction mixture of terpy with $RuCl_3{\cdot}H_2O$. The structure was confirmed by X-ray crystallography. Table 1 contains selected bond lengths and dihedral angles for [terpyH]PF_6. Table 2 displays crystallographic data and the ORTEP geometry of [terpyH]PF_6 is shown in Fig. 1. The proton at the central pyridine nitrogen atom N2 was not assumed in calculated positions but was found in electron density difference map. The protonated nitrogen N2 of the central pyridine ring is intramolecularly hydrogen-bonded to the adjacent pyridine-N atom (N1) of ring A (refer Scheme 1). Although the pyridine rings A and B in the neutral (free) terpy are inclined toward the central pyridine ring by 37.0° (the calculated value), the protonated form of [terpyH]$^+$ has almost planar pyridine rings; the pyridine rings A and B are inclined toward the central pyridine ring by only 0.8 and 179.3°, respectively.

A projection of the crystal packing of [terpyH]PF_6 along the *b*-axis is shown in Fig. 2. The H atom on the C16 position of [terpyH]PF_6 is involved in a hydrogen bond consisting of an intramolecular C—H---F = 2.378 Å and ∠C—H---F = 164.47°. The H atom on the N2 position of [terpyH]PF_6 is also involved in a

Table 1. Comparison of calculated bond lengths and dihedral angles for compound **1** with experimental values from X-ray diffraction[a]

	Distances (Å)			Dihedral angle (°)	
	calc.	exp.		calc.	exp.
N1–C5	1.341	1.367(8)	N1–C5–C6–N2	1.60	0.6(10)
C5–C6	1.480	1.468(10)	N2–C10–C11–N3	1.60	179.3(7)
N2–C6	1.353	1.312(8)			
N2–C10	1.353	1.345(9)			
C10–C11	1.480	1.470(9)			
N3–C11	1.341	1.353(9)			

[a] The atom numbering is shown in Fig. 1.

Table 2. Crystallographic data of **1**

Formula	$C_{15}H_{12}N_3PF_6$(**1**)
Formula weight	379.24
Crystal system	Monoclinic
Space group	*P2/n*
a/Å	11.991(2)
b/Å	6.4497(9)
c/Å	21.149(3)
α/deg	90
β/deg	107.616(3)
γ/deg	90
Z	4
λ(MoKα)	0.71069
θ_{max}	27.5
h	−15 to 15
k	−8 to 8
l	−27 to 27
μ/cm^{-1}	2.46
Dc/Mgm^{-3}	1.616
T/K	296
V/Å^3	1558.9(4)
R_1	0.118
R_w	0.279

weak hydrogen bond consisting of an intermolecular N2—H---F bond of 2.644 Å, and ∠N2—H---F = 156.85°. Analysis of the crystal packing showed that there is intermolecular short contact between the adjacent pyridine-N atom (N3) of ring B and hydrogen of another [terpyH]PF_6. The distance between the N3 and H is 2.507 Å and the angle ∠C—H---N3 160.63°. This distance

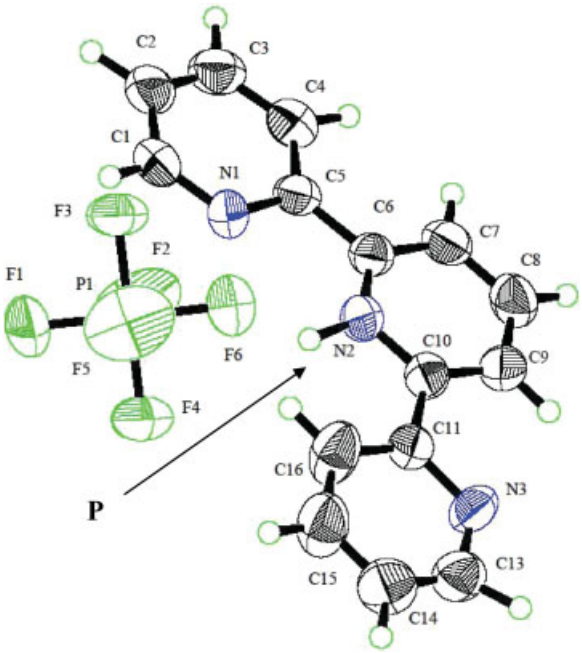

Figure 1. Molecular structure of [terpyH]PF_6 (**1**). Thermal displacement ellipsoids are drawn at the 50% probability level. P denotes the attached proton

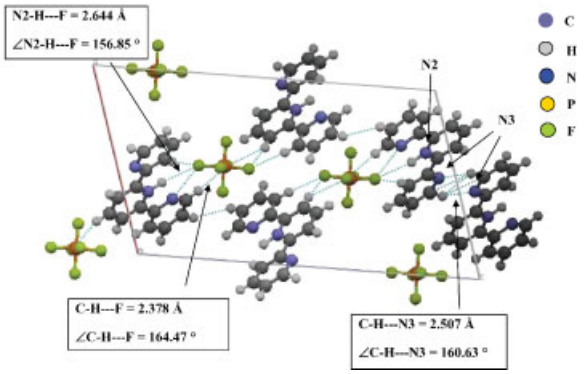

Figure 2. A projection of the crystal packing of [terpyH]PF_6 along the *b*-axis

is short enough to restrict the rotation of pyridine ring B (refer Scheme 1).

Part of the crystal packing of [terpyH]CF_3SO_3 reported[19] is shown in the bottom of Fig. 3(b). The planar terpy moieties are aligned parallel to each other, which are stacked with sets of parallel planes. This distribution consists of a set of planar arrays at a distance of 3.135 Å. There is the extensive hydrogen-bonding network among molecules together with strong dipole–dipole interactions.

On the other hand, part of the crystal packing of [terpyH]PF_6 in the present work is shown in Fig. 3(a). This packing is not similar to previous one.[19,20] The figure of [terpyH]PF_6 indicates a random packing with dihedral angle of 60.91°, which suggests that strong hydrogen-bonding interactions are absent among $[terpyH]^+$ molecules.

Absorption property

The differences in the absorption spectral properties between terpy and [terpyH]PF_6 were studied. Figure 4 shows the absorption spectra of terpy and [terpyH]PF_6 in CH_3CN solution.

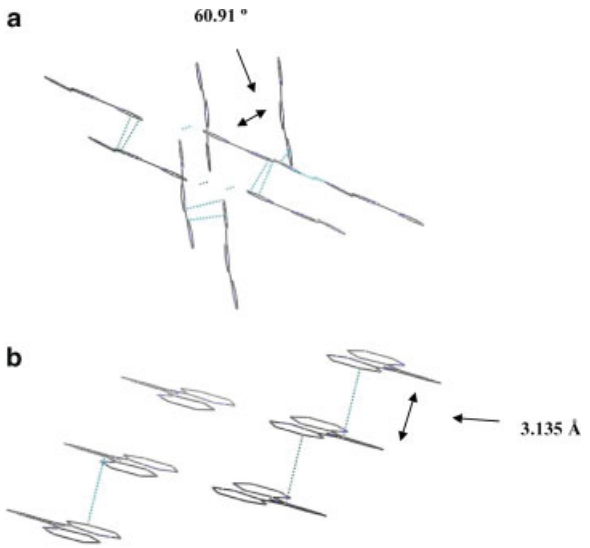

Figure 3. Part of the crystal packing. (a) [terpyH]PF_6, (b) [terpyH]CF_3SO_3.[19] For the sake of clarity, H atoms bonded to C atoms have been omitted

Journal of Physical Organic Chemistry

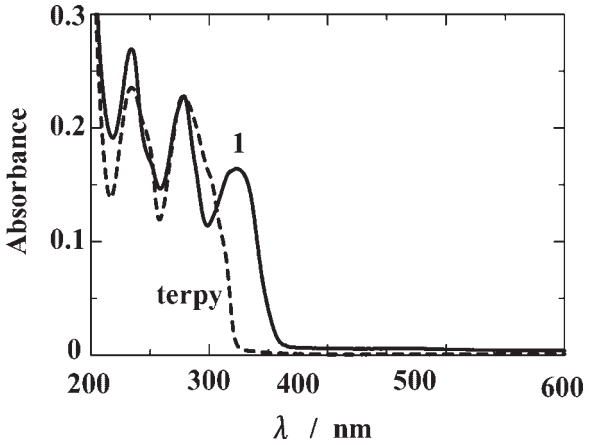

Figure 4. Electronic absorption spectra of **1** (solid line) and terpy (dotted line) in CH_3CN solution (1.0×10^{-5} M) at 25 °C

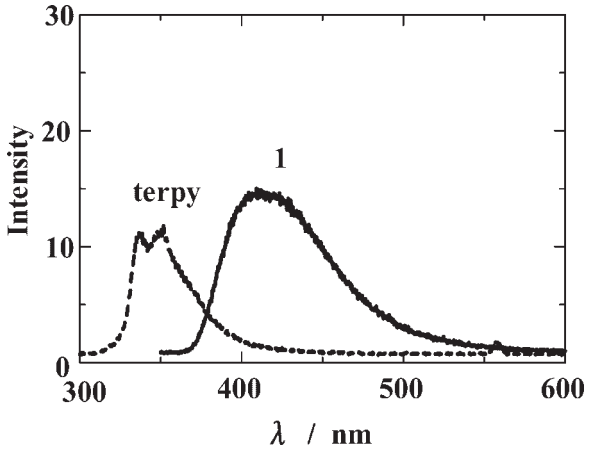

Figure 5. Emission spectra of **1** (solid line) and terpy (dotted line) ($\lambda_{ex} = 278$ nm) in CH_3CN solution (1.0×10^{-5} M) at 25 °C

Table 3. Absorption and emission properties of 1 and terpy in CH_3CN at 25 °C

Compound	Absorption λ_{max}/nm ($\varepsilon/10^3$ M^{-1} cm^{-1})			Electrochemistry/V reduction	Emission λ_{em}/nm	τ/ns	Φ^a
[terpyH]PF_6(1)	234 (0.234)	278 (0.228)	316 (0.163)	−0.62	412	25.6	0.052
terpy	234 (0.234)	278 (0.260)		−2.12	340		

[a] The emission quantum yield was determined at room temperature relative to those of a solution containing $[Ru(bpy)_3]^{2+}$ ($\Phi = 0.062$) and having the same absorbance.

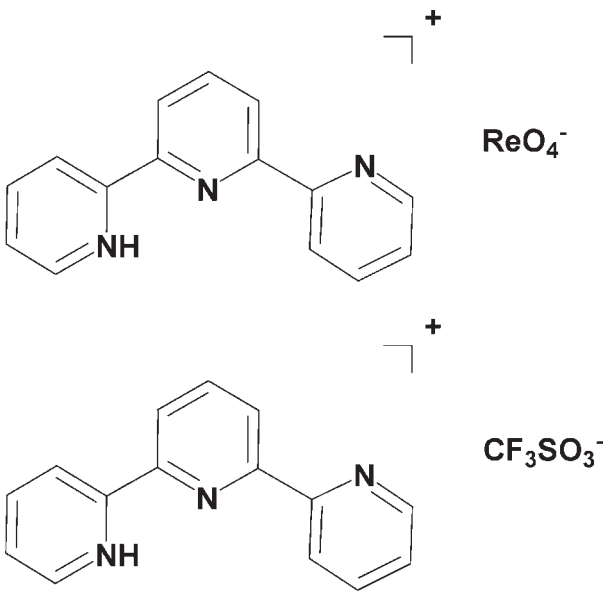

Scheme 2. The mono-protonated forms reported so far

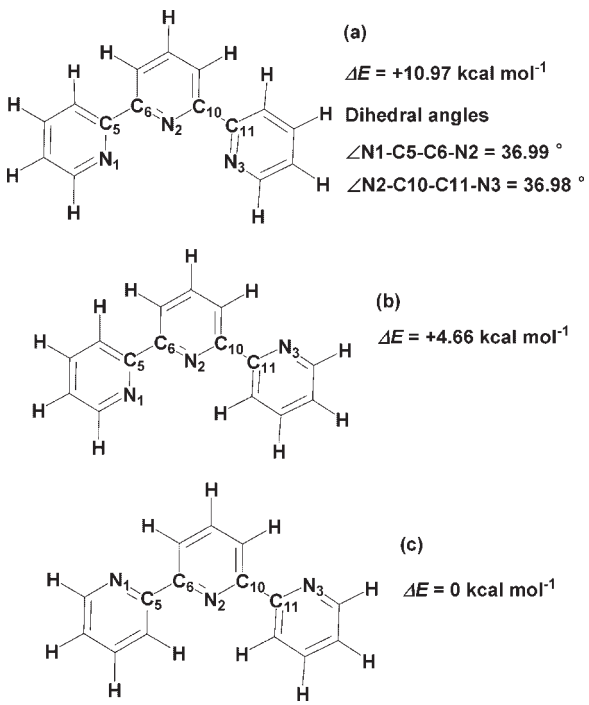

Figure 6. Calculated geometries of three isomers of terpy. ΔE is the relative energy by RB3LYP/6-311+G (3df,2p)//B3LYP/6-31G* ZPE. (a) and (b) are the less favorable geometry and (c) is the most favorable geometry

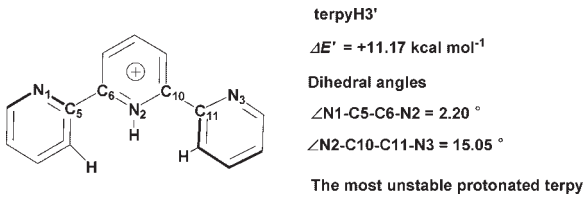

Scheme 3. The most unstable protonated terpyridine, terpyH3′

The absorption maxima and molar absorption coefficients are listed in Table 3. In Fig. 4, [terpyH]PF_6 (solid line) and terpy (dotted line) show strong and narrow absorption bands at 234 and 278 nm, respectively, which are assigned to the π–π^* transition of terpy. [terpyH]PF_6 also has a strong band at 316 nm, being assigned to a π–π^* transition. Such a red-shifted and new π–π^* transition in the band maximum of [terpyH]PF_6 can be ascribed to the π delocalization due to the planarity of the protonated terpy.

Electrochemical and emission properties

Table 3 also summarizes electrochemical data of [terpyH]PF_6 and terpy obtained from CV. [terpyH]PF_6 and terpy do not display an oxidation peak in the potential window. The reduction potential of [terpyH]PF_6 ($E_{red} = -0.62$ V) is more positive than that of terpy ($E_{red} = -2.12$ V), indicating strong effect of the proton on descent of the LUMO energy of terpy. Next, the emission maxima and the excited-state lifetimes of [terpyH]PF_6 are shown in Table 3. The symbols λ_{max} and λ_{em} are the absorption and emission wavelengths, respectively. [terpyH]PF_6 showed an intense blue

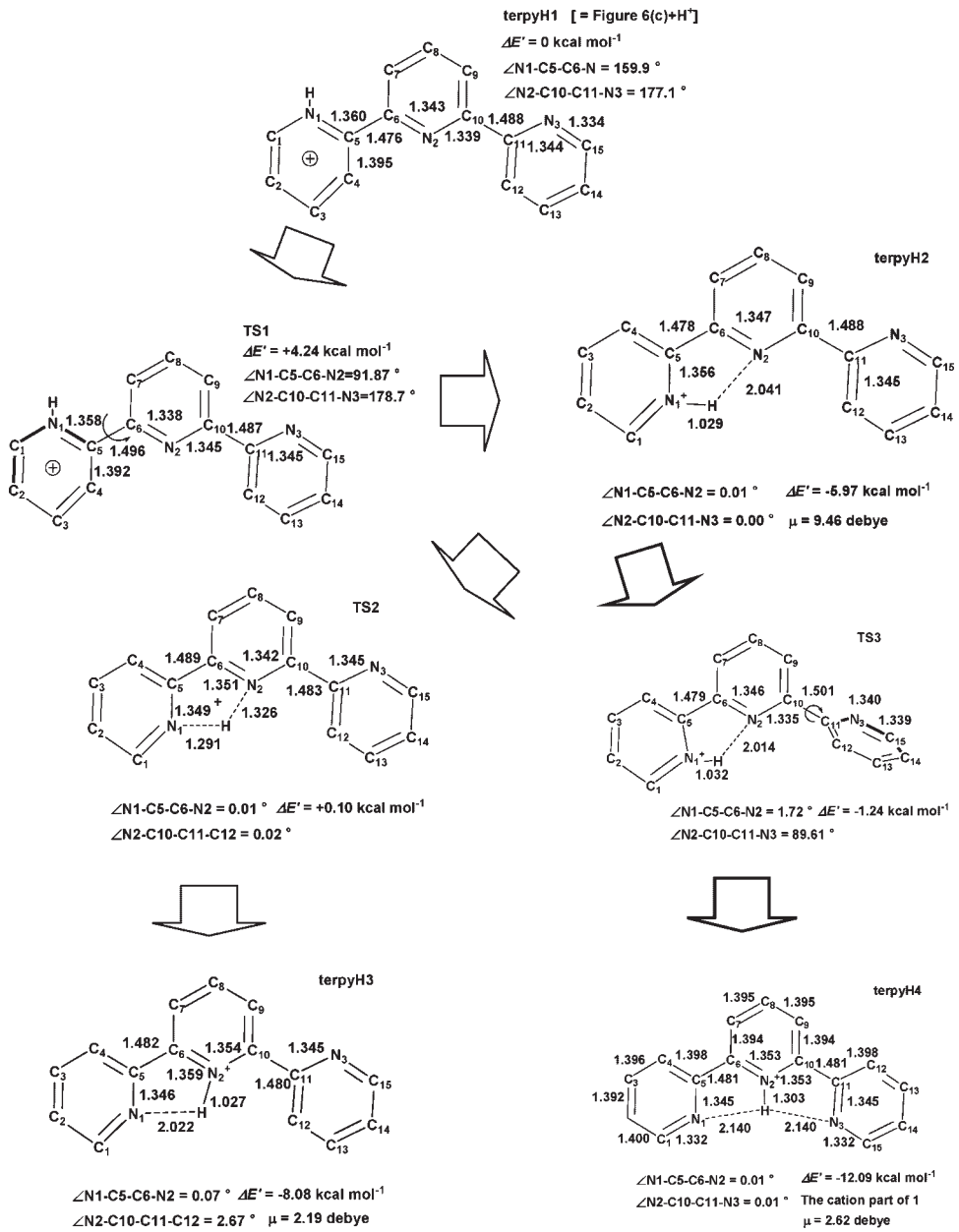

Figure 7. Isomerization paths of the protonated terpyridine (termed terpyH). TS is the transition state. Distances are in Å. $\Delta E'$ is the B3LYP/6-311+G (3df,2p)//B3LYP/6-31G* ZPE energy difference relative to that of terpyH1. That is, the more $\Delta E'$ value corresponds to the less stable isomer. Hydrogen atoms except the proton are omitted in geometric figures. Atom numbering is the same as that in Fig. 1. μ is the calculated dipole moment

emission at 412 nm ($\Phi = 0.052$ in CH_3CN at room temperature) without a central metal ion (Fig. 5). The protonation shifted the band maximum to the longer wavelength relative to that of the free terpy ($\lambda_{em} = 340$ nm). Thus, the π delocalization due to the planarity of the protonated terpy is essential for the intense blue emission.

Computational results

Two mono-protonated terpyridine salts have been reported to have the *cis–trans*-conformation of the pyridine rings (Scheme 2).[19,20] In contrast, the present [terpyH]PF_6 is of the central protonation and the PF_6^- anion is located distantly as indicated in Fig. 1. The stability and the protonation pathways were examined by using DFT calculations. The stable geometry of terpy was firstly investigated. Figure 6 shows three geometric isomers of the neutral terpy. Here, ΔE is the energy difference and the more positive value of ΔE indicates the less stable form. Thus, the isomer (c) is the most stable form, where three nitrogen lone-pair orbitals expand in different directions resulting in the smallest exchange repulsion. Next, the protonation to the isomer (c) of terpy is considered. The in-plane central protonation is unfavorable owing to the steric repulsion by two *ortho* protons. In fact, the protonated form (terpyH3 in Scheme 3) has the most unstable geometry among all of isomers (terpyH1, terpyH2, and terpyH3). Thus, the protonation should occur not at the central N2 atom but at the peripheral one (N1 or N3). The protonated species, terpyH1, is shown in the top of Fig. 7. The protonated pyridine ring can rotate via a rotation TS (TS1) to give the first isomer (terpyH2) of the protonated terpy. The isomer terpyH2 is -5.97 kcal mol^{-1} more stable than terpyH1, and the activation energy of TS1 is small (4.24 kcal mol^{-1}). The species terpyH2 corresponds to the cation fragment in Scheme 2. In the molecular structure of the [terpyH]CF_3SO_3, the $CF_3SO_3^-$ anion is located to the asymmetry position of [terpyH]$^+$ cation.[19] The second rotation of terpyH2, TS3, was obtained, which leads to a symmetric form (terpyH4). This species is more stable (-12.09 kcal mol^{-1}) than terpyH1. However, terpyH4 is not a component of the present crystal structure. Therefore, it is suggested that TS3 is prohibited in the solid state, although it is likely in the gas phase. The prohibition comes from intermolecular short contact between the adjacent pyridine-N atom (N3) of ring B. Besides TS3, TS2 was found via the in-plane proton shift transition state. The tautomerization leads to terpyH3 which is a component of the present crystal structure. The tautomer terpyH3 is slightly more stable ($\Delta E' = -8.08$ kcal mol^{-1}) than terpyH2 ($\Delta E' = -5.97$ kcal mol^{-1}).

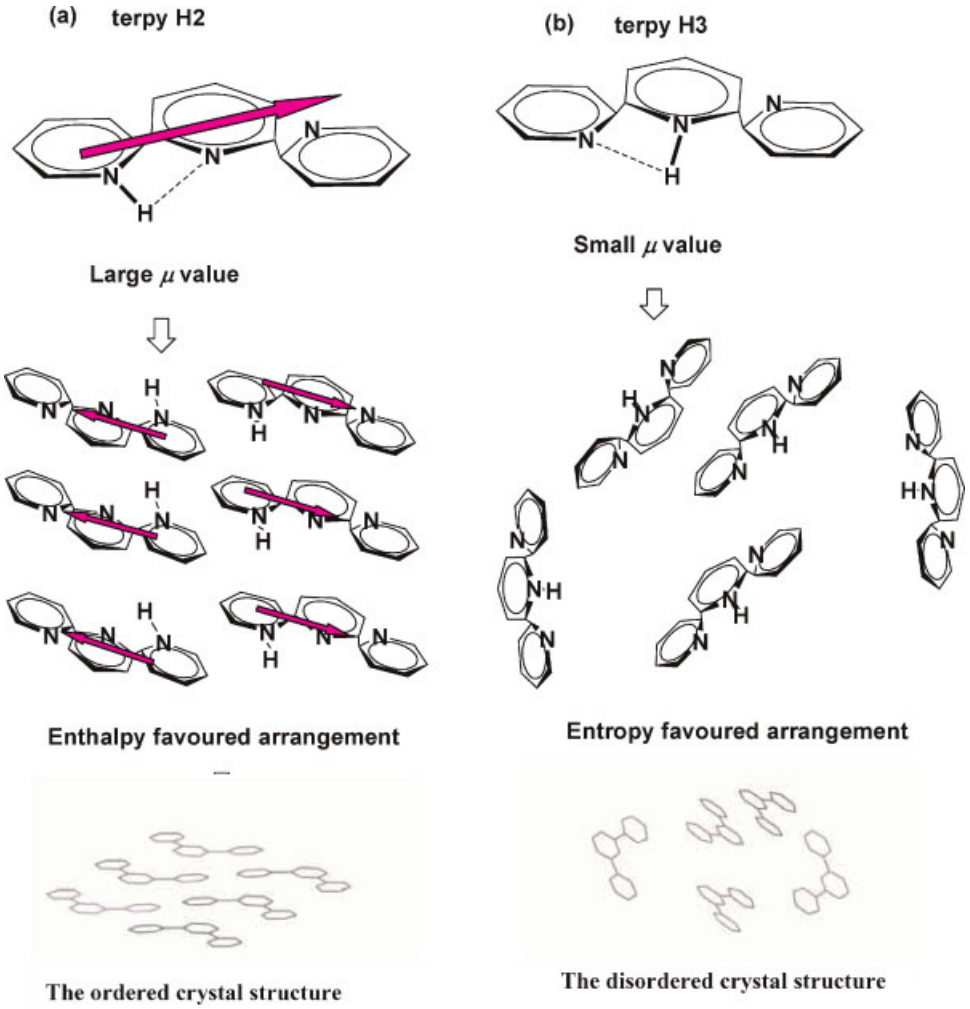

Scheme 4. A slight difference of the proton positions in terpyH gives a drastic difference in crystal pattern. Direction of arrows of the dipole-moment vectors comes from the Cartesian components, $\mu_x = -9.107$ D and $\mu_y = -2.559$ D

It is significantly questionable why both terpyH2 based[19,20] and terpyH3 based structures were obtained in crystal structures.

Correlation of the tautomeric form of terpyH and the aggregation pattern

Our terpyH3 based crystal structure is in contrast with the terpyH2 based regularly arranged one.[19,20] The drastic difference may come from that of the polarity of terpyH2 and terpyH3. The dipole moment of terpyH2 was calculated to be 9.46 D, while that of terpyH3 is 2.19 D. The anti-parallel orientation of two terpyH2 units gives rise to a large permanent dipole–dipole attraction energy, $U(r)$:[21]

$$U(r) = \frac{-2{\mu_1}^2 \cdot {\mu_2}^2}{(4\pi\varepsilon_0)^2 \cdot 3kT \cdot r^6}$$

Here μ is the dipole moment, ε_0 the dielectric constant, k the Boltzmann constant, T the absolute temperature, and r the distance. $U(r = 3.1\ \text{Å})$ for the dimer $(\text{terpyH2})_2$ is 16.88 kcal mol^{-1}, while $U(r = 2.9\ \text{Å})$ for the dimer $(\text{terpyH3})_2$ is 0.072 kcal mol^{-1}. Although terpyH2 is itself at the quasi-stable state, the dipole–dipole interaction stabilizes the terpyH2 species.

The left side of Scheme 4 exhibits the process of aggregation of the terpyH2 component. The ordered crystal structure is completed by accumulation of the permanent dipole–dipole interactions. Stacking structure both of the anti-parallel orientation by permanent dipole–dipole interaction and in the small steric crowd is shown. On the other hand, the component terpyH3 has a small dipole moment and cannot undergo effective molecular interactions. With small molecular interaction and no energetic stability during the aggregation, the random, that is, entropy favored arrangement is gained. Each terpyH3 component is obligated to be situated so that the random orientation may give rise to the $-T\Delta S$ stability in $\Delta G = \Delta H - T\Delta S$. It is surprising that the very slight difference of proton positions in the tautomeric form (terpy H2 and terpy H3) gives significant effect on crystal structures.

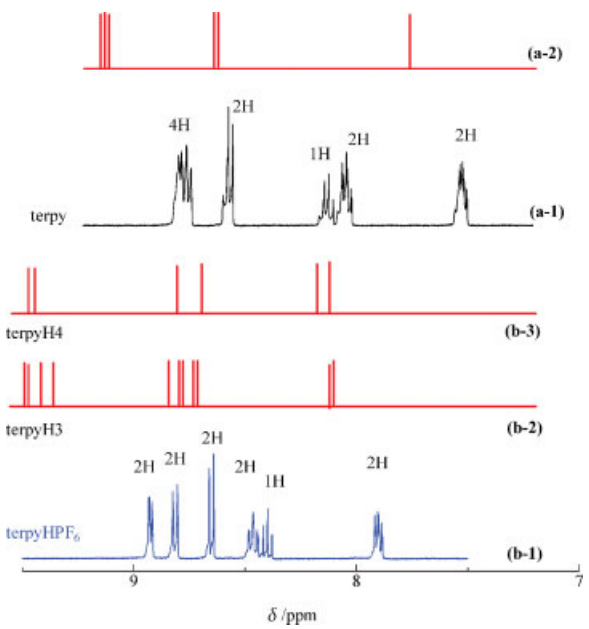

Figure 8. ^{1}H NMR spectra of terpy, (a-1), and terpyHPF$_6$, (b-1), in CD_3CN. (a-2) shows chemical shifts of GIAO SCRF = PCM calculations of terpy. (b-2) exhibits those of terpyH3 and (b-3) does those of terpyH4, respectively

^{1}H NMR chemical shifts of 1 in CD_3CN solution

Since the isomer terpy H4 is more stable than terpy H3 (Fig. 7), the former might be present in solutions. Figure 8(a-1) shows the ^{1}H NMR spectra of terpy in CD_3CN. In accordance of the C_{2v} geometry in Fig. 6(c), there are six groups of chemical shifts. They can be assigned to respective protons by aid of GIAO calculations. The observed chemical shifts are somewhat different from those of GIAO calculations. The difference would come from the solute–solvent molecular interactions involved in the solution for the NMR measurement. Aside from the difference, the trend and the sequence of the shifts are similar. Figure 8(b-1) shows the spectrum of the protonated terpy. There are seven groups of shifts, which is consistent with terpyH4 of the C_{2v} symmetry in Fig. 8(b-3) rather than with terpyH3 in Fig. 8(b-2). Thus, the computational result that terpyH4 is more stable than terpyH3 was confirmed under the condition that constraint for the pyridine-ring rotation is relaxed.

SUMMARY

In this work, 2,2′:6′,2″-terpyridinium hexafluorophosphate where the proton is attached to the central nitrogen atom was synthesized and its crystal structure was determined. The protonated species has a specific absorption band at $\lambda_{max} = 316$ nm and a strong blue emission at $\lambda_{em} = 412$ nm. The absorption and emission spectral features were brought about by extension of the π conjugation by protonation of terpy. CV for the proton adduct showed the first reduction wave at around -0.6 V, being more positive than that of the neutral species. Finally, isomerization process of the central protonated form was examined via the side protonated one. The molecular arrangement in the crystal structure is entirely different from those reported so far.[19,20] The slight difference of proton positions of the tautomers gives a drastic difference of crystal patterns. The isomer of protonated terpy in the solid state (terpyH3) is different from that in the solution state (terpyH4).

Acknowledgements

This research was partly supported by Grant-in-Aid for Scientific Research No. 19550064 (K. T.) from the Ministry of Education, Culture, Sports, and Science and Technology (MEXT) of Japanese Government.

REFERENCES

[1] V. Balzani, A. Juris, N. Venturi, S. Campagna, S. Serroni, *Chem. Rev.* **1996**, *96*, 759.
[2] M. Maestri, N. Armaroli, V. Balzani, E. C. Constable, A. M. W. Cargill Thompson, *Inorg. Chem.* **1995**, *34*, 2759.
[3] A. Dovletoglou, S. A. Adeyemi, T. J. Meyer, *Inorg. Chem.* **1996**, *35*, 4120.
[4] K. Hutchison, J. C. Morris, T. A. Nile, J. L. Walsh, *Inorg. Chem.* **1999**, *38*, 2516.
[5] N. Yoshikawa, S. Yamabe, N. Kanehisa, Y. Kai, H. Takashima, K. Tsukahara, *Inorg. Chim. Acta* **2006**, *359*, 4585.
[6] M. Graf, H. S. Evans, *Acta Crystallogr. C* **1996**, *52*, 3073.

[7] M. G. B. Drew, M. J. Hudson, P. B. Iveson, M. L. Russel, J. O. Liljenzin, M. Skaberg, L. Spijuth, C. Madic, *J. Chem. Soc., Dalton Trans.* **1998**, 2973.
[8] C. Berthon, M. S. Grigoriev, *Acta Crystallogr. E* **2005**, *61*, 1216.
[9] N. Yoshikawa, T. Matsumura-Inoue, N. Kanehisa, Y. Kai, H. Takashima, K. Tsukahara, *Anal. Sci.* **2004**, *20*, 1639.
[10] P. A. Anderson, L. F. Anderson, M. Furue, P. C. Junk, F. R. Keene, B. T. Patterson, B. D. Yeomans, *Inorg. Chem.* **2000**, *39*, 2721.
[11] N. Yoshikawa, A. Ichimura, N. Kanehisa, Y. Kai, H. Takashima, K. Tsukahara, *Acta Crystallogr. E* **2005**, *61*, m55.
[12] G. M. Sheldrick, SHELXL 97, University of Göttingen, Germany, **1997**.
[13] M. J. Frisch, G. W. Trucks, H. B. Schlegel, G. E. Scuseria, M. A. Robb, J. R. Cheeseman, V. G. Zakrzewski, J. A. Montgomery, Jr., R. E. Stratmann, J. C. Burant, S. Dapprich, J. M. Millam, A. D. Daniels, K. N. Kudin, M. C. Strain, O. Farkas, J. Tomasi, V. Barone, M. Cossi, R. Cammi, B. Mennucci, C. Pomelli, C. Adamo, S. Clifford, J. Ochterski, G. A. Petersson, P. Y. Ayala, Q. Cui, K. Morokuma, D. K. Malick, A. D. Rabuck, K. Raghavachari, J. B. Foresman, J. Cioslowski, J. V. Ortiz, A. G. Baboul, B. B. Stefanov, G. Liu, A. Liashenko, P. Piskorz, I. Komaromi, R. Gomperts, R. L. Martin, D. J. Fox, T. Keith, M. A. Al-Laham, C. Y. Peng, A. Nanayakkara, C. Gonzalez, M. Challacombe, P. M. W. Gill, B. Johnson, W. Chen, M. W. Wong, J. L. Andres, C. Gonzalez, M. Head-Gordon, E. S. Replogle, J. A. Pople, GAUSSIAN 98, revision A.7, Gaussian Inc., Pittsburgh PA, **1998**.
[14] A. D. Becke, *J. Chem. Phys.* **1993**, *98*, 5648.
[15] C. Lee, W. Yang, R. G. Parr, *Phys. Rev. B* **1988**, *37*, 785.
[16] J. B. Foresman, A. E. Frisch, *Exploring Chemistry With Electronic Structure Methods* (2nd edn), Gaussian, Inc., Pittsburgh, PA, **1996**. Chapter 7.
[17] K. Wolinski, J. F. Hinton, P. Pulay, *J. Am. Chem. Soc.* **1990**, *112*, 8251.
[18] M. T. Cances, B. Mennucci, J. Tomasi, *J. Chem. Phys.* **1997**, *107*, 3032.
[19] A. Hergold-Brundic, Z. Popovic, D. Matkowic-Calgovic, *Acta Crystallogr. C* **1996**, *52*, 3154.
[20] A. Kochel, *Acta Crystallogr. E* **2006**, *62*, m37.
[21] D. A. McQuarrie, J. Simon, *Physical Chemistry, a Molecular Approach*, University Science Books, California, CA, **1997**. Chapter.16.

